DOI 10.1002/mnfr.200900115 *Mol. Nutr. Food Res.* 2010, *54*, 566–575

RESEARCH ARTICLE

Angiostatic effects of Brazilian green propolis and its chemical constituents

Yuichi Chikaraishi[1], Hiroshi Izuta[1], Masamitsu Shimazawa[1], Satoshi Mishima[2] and Hideaki Hara[1]

[1] Department of Biofunctional Evaluation, Molecular Pharmacology, Gifu Pharmaceutical University, Gifu, Japan
[2] Nagaragawa Research Center, Api Co. Ltd., Gifu, Japan

Received: March 16, 2009
Revised: May 28, 2009
Accepted: June 12, 2009

Propolis, a resinous substance collected by honeybees from various plant sources, has several pharmacological actions, such as anti-tumor and anti-inflammatory effects. The aim of this study was to evaluate the anti-angiogenic effects of a water extract of Brazilian green propolis (WEP) and its constituents, caffeoylquinic acid derivatives, against angiogenic processes in human umbilical vein endothelial cells (HUVECs) *in vitro*. We also examined the anti-angiogenic effects of WEP against retinal neovascularization in a murine oxygen-induced retinopathy model *in vivo*. WEP and its constituents significantly suppressed vascular endothelial growth factor (VEGF)-induced HUVEC proliferation, migration, and tube formation *in vitro*. WEP and its caffeoylquinic acid derivatives suppressed VEGF-stimulated phosphorylation of mitogen-activated protein kinase in HUVECs (*versus* VEGF alone). Moreover, WEP (300 mg/kg/day, subcutaneously for 5 days) significantly suppressed retinal neovascularization in the murine oxygen-induced retinopathy model. These data indicate that (i) WEP has angiostatic effects against angiogenic processes *in vitro* and in an *in vivo* model of murine oxygen-induced retinopathy and (ii) the inhibitory effects of WEP against *in vitro* angiogenesis are chiefly derived from its caffeoylquinic acid derivatives. Judging from these findings, WEP and its caffeoylquinic acid derivatives may represent candidates for preventive or therapeutic agents against diseases caused by angiogenesis.

Keywords:
Caffeoylquinic acid / Human umbilical vein endothelial cells / Mice / Oxygen-induced retinopathy / Propolis

1 Introduction

Propolis, a resinous substance collected by honeybees from various plant sources, is used by the bees to protect the nest entrance against intruders and bacteria, and to seal holes in their honeycombs. It has been used as a traditional folk medicine from ancient times in many countries. More recently, it has been demonstrated to have a wide range of pharmacological actions, such as antibacterial [1, 2], anti-inflammatory [3], and anti-tumor activities [4, 5]. Propolis contains numerous biochemical constituents, including cinnamic acids, benzoic acids and their esters, substituted phenolic acids and esters, flavonoids, and amino acids [6–8]. The properties and constituents of propolis vary with its geographical origin [9], and the differences in its constituents are basically due to differences in the plants from which it is sourced [10]. *Baccharis dracunculifolia* DC (Asteraceae), a plant native to Brazil, is the most important botanical source of Southeastern Brazilian propolis, known as green propolis because of its color [11–15].

Angiogenesis, the formation of new vessels from pre-existing endothelium, is an important process because it

Correspondence: Professor Hideaki Hara, Department of Biofunctional Evaluation, Molecular Pharmacology, Gifu Pharmaceutical University, 5-6-1 Mitahora-higashi, Gifu 502-8585, Japan
E-mail: hidehara@gifu-pu.ac.jp
Fax: +81-58-237-8596

Abbreviations: 3,4-CQA, 3,4-di-*O*-caffeoylquinic acid; **3,5-CQA,** 3,5-di-*O*-caffeoylquinic acid; **ChA,** chlorogenic acid; **CoA,** *p*-coumaric acid; **ERK,** extracellular signal-regulated kinase; **HUVECs,** human umbilical vein endothelial cells; **MAPK,** mitogen-activated protein kinase; **p38,** p38 MAPK; **VEGF,** vascular endothelial growth factor; **WEP,** water extract of Brazilian green propolis; **WST-8,** 2-(2-methoxy-4-nitrophenyl)-3-(4-nitrophenyl)-5-(2,4-disulfophenyl)-2H-tetrazolium

supports the increasing demands for metabolic supplies (nutrients, various growth factors, and molecular oxygen to sites of tissue repair or regeneration) during embryonic development, endometrial and placental proliferation, wound healing, and revascularization of ischemic tissues. However, uncontrolled and excessive angiogenesis (neovascularization) is a central feature of cancer, rheumatoid arthritis, and atherosclerosis. In the ophthalmological field, ocular neovascularization is known to occur in various parts of the eye, such as the cornea, iris, retina, and choroid. Some of these regional types of neovascularization (especially retinal and subretinal (choroidal) neovascularization, which are characteristics of diseases such as diabetic retinopathy, the retinopathy of prematurity, and age-related macular degeneration) are leading causes of irreversible failing vision and blindness worldwide.

It is known that vascular endothelial growth factor (VEGF) activates various mitogen-activated protein kinases (MAPKs) through the VEGFR-2 downstream pathway. VEGF-mediated endothelial cell proliferation is promoted by the classical Ras-dependent signaling cascade impinging extracellular signal-regulated kinase (ERK) 1/2 [16]. On the other hand, VEGF-induced endothelial cell migration is mediated by (MAPK p38) p38 [17].

Recently research reports have disclosed anti-angiogenic effects of propolis. For example, Song *et al.* [18] noted inhibitory effects of an ethanol and ether extract of Korean propolis in a chick embryo chorioallantoic membrane assay and in a calf pulmonary arterial endothelial cell proliferation assay (both *in vivo* and *in vitro*). Hepsen *et al.* [19] reported that topical application of a water extract of Turkish propolis has an inhibitory effect on the corneal neovascularization that occurs following silver nitrate cauterization in rabbits *in vivo*. However, to our knowledge, no study has examined the effects of caffeoylquinic acid derivatives toward angiogenesis both *in vitro* and *in vivo*. In this study, we examined the effects of water extract of Brazilian green propolis (WEP) and its major constituents on various steps involved in VEGF-induced angiogenesis (proliferation, migration, and tube formation) in human umbilical vein endothelial cells (HUVECs). Moreover, we examined the effects of WEP on retinal neovascularization in a murine oxygen-induced retinopathy model.

2 Materials and methods

2.1 Materials

HUVECs, endothelial cell basal medium (HuMedia-EB2), and VEGF were purchased from Kurabo (Osaka, Japan). Collagen type I (Cellmatrix type I-C) was from Nitta Gelatin (Osaka, Japan), *p*-coumaric acid (CoA) was from Sigma-Aldrich (St. Louis, MO, USA) and 3-caffeoylquinic acid (chlorogenic acid (ChA)) was from TC1 TOKYO KASEI (Tokyo, Japan). Artepillin C, baccharin, drupanin, 3,4-di-*O*-caffeoylquinic acid (3,4-CQA), 3,5-di-*O*-caffeoylquinic acid (3,5-CQA), and WEP were kindly provided by Dr. Kazumichi Suzuki of Api (Gifu, Japan). Anti-phosphorylated ERK 1/2 (Thr202/Tyr204), anti-total ERK 1/2, anti-total p38, or anti-β-actin antibody was from Cell Signaling Technology (Beverly, MA, USA). Anti-phosphorylated p38 antibody was from Promega (Madison, WI, USA). Brazilian green propolis (Minas Gerais state, Brazil), which originates mainly from *B. dracunculifolia* [14], was extracted with water at 50°C to yield the extract used here (WEP). The main constituents of WEP were previously reported by Mishima *et al.* [20], and the concentrations used in the present *in vitro* tube formation are summarized in Table 1.

2.2 Cell culture

HUVECs were cultured in growth medium HuMedia-EG2 at 37°C in a humidified atmosphere of 5% CO_2 in air. The HuMedia-EG2 medium consists of HuMedia-EB2 supplemented with 2% FBS, 10 ng/mL human epidermal growth factor, 5 ng/mL human fibroblast growth factor B, 1 μg/mL hydrocortisone, 10 μg/mL heparin, 50 ng/mL amphotericin B, and 50 μg/mL gentamicin. Subconfluent monolayers of HUVECs, from passages 3 to 5, were used in the experiments.

2.3 *In vitro* tube formation assay

An angiogenesis assay kit (Kurabo) was used according to the manufacturer's instructions. This kit consists of a 24-well cluster dish in which HUVECs and fibroblasts had been seeded under the optimal condition for capillary tube formation. The culture medium in each well was changed with fresh medium containing VEGF (10 ng/mL) and various concentrations of WEP or its constituents (Table 1) on days 1, 4, 7, and 9. The WEP was dissolved in distilled water, whereas its constituents were each dissolved in DMSO. DMSO, to a final concentration of 0.1% in each examination, was added to WEP, the non-drug control, and VEGF alone. On day 11, cells were fixed in 70% ethanol and stained with anti-CD31 antibody. For the evaluation of capillary tube formation (the stained tube-like structures), five different photographs were taken for each well using a digital camera (Coolpix 4500; Nikon, Tokyo, Japan). These photographs were used for measurement of the tube area (the total area of the tubes), tube length (the total length of the tubes), joints (the number of capillary connections), and paths (the number of tubes branching from the capillary-like network) of the stained tube-like structures by means of an angiogenesis image analyzer version 2 (Kurabo).

Table 1. Major constituents present in WEP, and the concentrations used in the present *in vitro* tube formation[a)]

Constituents	Content in WEP (%)	Concentration (μM)/ WEP (100 μg/mL)	Concentrations used in the present *in vitro* study (μM)
Caffeoylquinic acid derivatives			
3,4-Di-*O*-caffeoylquinic acid (3,4-CQA)	6.1	11.8	10.0
3,5-Di-*O*-caffeoylquinic acid (3,5-CQA)	4.9	9.5	10.0
chlorogenic acid (ChA)	3.6	10.2	10.0
Cinnamic acid derivatives			
p-Coumaric acid (CoA)	3.7	22.6	20.0
Artepillin C	0.59	2.0	2.0
Drupanin	0.12	0.5	0.5
Baccharin	0.03	0.1	0.1

a) Data in this table are partially modified from [20].

2.4 *In vitro* cell proliferation assay

Subconfluent (~80%) HUVECs were trypsinized, seeded into a 96-well plate at 2000 cells/well, and incubated in HuMedia-EG2 medium (growth medium) for 24 h. The culture medium was then changed to HuMedia-EB2 with 2% FBS (basal medium), and incubation allowed to proceed for 24 h. The culture medium was then changed to basal medium containing VEGF (10 ng/mL; Kurabo) with or without a given concentration of WEP or a caffeoylquinic acid derivative (3,4-CQA, 3,5-CQA, or ChA), and incubation continued for a further 72 h. Cell proliferation was estimated by measuring cell metabolic activity using a Cell Counting Kit-8 (Dojindo, Kumamoto, Japan) according to the manufacturer's instructions. The viable cell numbers were measured using a water-soluble tetrazolium salt, 2-(2-methoxy-4-nitrophenyl)-3-(4-nitrophenyl)-5-(2,4-disulfophenyl)-2H-tetrazolium (WST-8) and 1-methoxy-phenazine methosulfate. At the end of the drug treatments, the culture medium was changed back to the basal medium. Then, 10 μL of WST-8 assay solution was added to each well, and incubation allowed to proceed for 4 h at 37°C. Finally, the absorbance of the culture medium at 450 nm was measured using a microplate reader (Varioskan® Flash, Thermo Electron, Vantaa, Finland).

2.5 *In vitro* wounding-healing assay

An *in vitro* wound-healing assay was performed to measure unidirectional migration by HUVECs. For this, we modified part of the procedure described by Izuta *et al.* [21]. Briefly, HUVECs (4×10^4/well) were seeded in 12-well plates coated with collagen type I, and incubated at 37°C until they attached. The HUVECs were then washed with PBS twice and incubated in Humedia-EB2 with 1% FBS for 24 h at 37°C. The monolayers of HUVECs were scratch-wounded to a 1-mm depth in a straight line using a 10–200-μL pipette tip, and incubated with VEGF (10 ng/mL) with or without a given concentration of WEP or a caffeoylquinic acid derivative (3,4-CQA, 3,5-CQA, or ChA) for 24 h. To measure the number of endothelial cells that had migrated from the edge of the injured monolayer, images were photographed both immediately after wounding and after 24-h incubation using a phase-contrast microscope (Olympus, Tokyo, Japan), about four points in each of three fields being taken at random in two independent wounds.

2.6 Western blot analysis

Subconfluent HUVECs were incubated in HuMedia-EB2 containing 2% FBS for 6 h at 37°C in a 5% CO_2 atmosphere. The medium was then changed to DMEM containing 25 mM HEPES (Invitrogen, Grand Island, NY, USA) and 2% FBS, and incubation allowed to proceed for a further 18 h at 37°C. Next, the medium was changed to fresh medium (25 mM HEPES included in DMEM) containing VEGF (10 ng/mL) with or without WEP (100 μg/mL) or 3,4-CQA (30 μM), and incubation continued for 5 min. Cells were washed with PBS, harvested, and lysed in RIPA buffer (Sigma) supplemented with protease inhibitor cocktail (Sigma) and phosphatase inhibitor cocktail 1 and 2 (Sigma). Lysates were centrifuged at $12\,000 \times g$ for 15 min at 4°C. Supernatants were collected and boiled for 5 min in SDS sample buffer (Wako). Equal amounts of protein were subjected to SDS-PAGE on a 10% gel, and then transferred to polyvinylidene difluoride membranes. After blocking with Block Ace (Snow Brand Milk Products, Tokyo, Japan) for 30 min, the membranes were incubated with the primary antibody (anti-phosphorylated ERK 1/2, anti-total ERK 1/2, anti-phosphorylated-p38 antibody, anti-total p38 antibody, or anti-β-actin antibody). After this incubation, the membrane was incubated with the secondary antibody (horseradish peroxidase-conjugated goat anti-rabbit IgG (Pierce Biotechnology, Rockford, IL, USA)). The immunoreactive bands

were visualized using Super Signal® West Femto Maximum Sensitivity Substrate (Pierce Biotechnology), and measured using GelPro (Media Cybernetics, Silver Spring, MD, USA). To measure the phosphorylation levels of ERK and p38, we normalized them with total ERK (t-ERK) and total p38 (t-p38), respectively.

2.7 Murine oxygen-induced retinopathy model

C57BL/6 mice (SLC, Shizuoka, Japan) were used. All investigations were performed in accordance with the ARVO statement for the use of animals in ophthalmic and vision research, and were approved and monitored by the Institutional Animal Care and Use Committee of Gifu Pharmaceutical University. The murine oxygen-induced retinopathy model was produced according to the protocol of Smith *et al.* [22]. Briefly, mouse pups (and their nursing mothers) were exposed to $75 \pm 1\%$ O_2 from postnatal day 7 (P7) to P12, the oxygen level in their cage being regulated and monitored by an oxygen controller (PRO-OX 110; Reming Bioinstruments, Redfield, NY, USA). On P12, they were returned to room air (21% O_2) until P17. WEP was freshly prepared each day just prior to administration. WEP was dissolved in PBS (vehicle) and was subcutaneously administered at 300 mg/kg/day for 5 days between P12 and P16. Within individual litters, animals were randomly assigned either to the vehicle ($n = 15$ from four litters) group or to the WEP group ($n = 14$ from four litters). At P17, the retinas were visualized by fluorescence angiography.

2.8 Fluorescence angiography

Mice were deeply anesthetized with 20 mg/kg sodium pentobarbital intraperitoneally (Nembutal; Dainippon-Sumitomo Pharmaceutical, Osaka, Japan). They were then perfused through the left ventricle with high molecular weight (MW = 2 000 000) fluorescein-conjugated dextran (Sigma-Aldrich) dissolved in PBS. After this perfusion, the eyes were enucleated and placed in 4% paraformaldehyde for 4–24 h. The cornea and lens were removed from each eye, and the retinas were dissected under a microscope. The flattened retinas were mounted using VECTASHIELD (Vector Laboratories, Burlingame, CA, USA).

2.9 Analysis of intraretinal angiogenesis and retinal neovascularization

We previously reported a method for measuring retinal neovascularization using imaging software (the Angiogenesis Tube Formation module in Metamorph) [23]. Briefly, total images of flat-mounted retinas were produced from 9 to 12 pieces of image acquired using a fluorescence microscope (BX50; Olympus) fitted with a × 4 microscope objective lens. Images were obtained using a high-resolution charge-coupled device camera (DP30BP; Olympus) *via* Metamorph (Universal Imaging, Downingtown, PA, USA). The three setting parameters (minimum tubule width, maximal tubule width, and intensity) in this software were set up, and each image was analyzed. We evaluated the number of nodes and the node area (parameters that are obtained from these analyzed images). Nodes are regions of ''connected blobs'', with their thickness exceeding the maximum width of the vessels, and are regions in which there is pooling of fluorescein-conjugated dextran. Such regions were shown as green labels in the analyzed images, and corresponded well to the pathological neovascularization area (including tortuous and dilated blood vessels, and abnormal vascular structures). To evaluate retinal revascularization, the capillary-free area was measured.

2.10 Statistical analysis

Data are given as mean ± SEM for the *in vitro* and *in vivo* studies, and as mean ± SD for the body weights of the mice. Statistical analysis was performed using a Student's *t*-test or Dunnett's multiple-comparison test, $p < 0.05$ being considered to indicate statistical significance.

3 Results

3.1 Effect on *in vitro* tube formation

Angiogenesis requires considerable behavioral activity among endothelial cells, including their proliferation, migration, and differentiation into tubular arrays (tube formation). To investigate the inhibitory effects of WEP and its constituents (3,4-CQA, 3,5-CQA, ChA, artepillin C, baccharin, CoA, and drupanin) on tube formation by endothelial cells *in vitro*, HUVECs and fibroblasts were co-cultured with VEGF (10 ng/mL) and/or various concentrations of WEP or its constituents. Each constituent was used at a concentration close to that present in a 100 μg/mL WEP solution, as indicated in Table 1. VEGF stimulated the formation of capillary-like structures by HUVECs, and this action was concentration dependently suppressed by addition of WEP (Fig. 1A). To evaluate tube formation by endothelial cells in a quantitative manner, four parameters (tube area, tube length, joints, and paths) obtained using an imaging analyzer were measured. WEP suppressed VEGF-induced tube formation by inhibiting each of the evaluated parameters (tube area, tube length, joints, and paths) in a concentration-dependent manner, each effect being significant at a concentration of 0.3 μg/mL or more (Figs. 1B–E). Artepillin C, baccharin, 3,4-CQA, 3,5-CQA, and ChA also significantly suppressed all four evaluated parameters, but CoA and drupanin significantly suppressed only the joints and paths parameters (Figs. 1B–E).

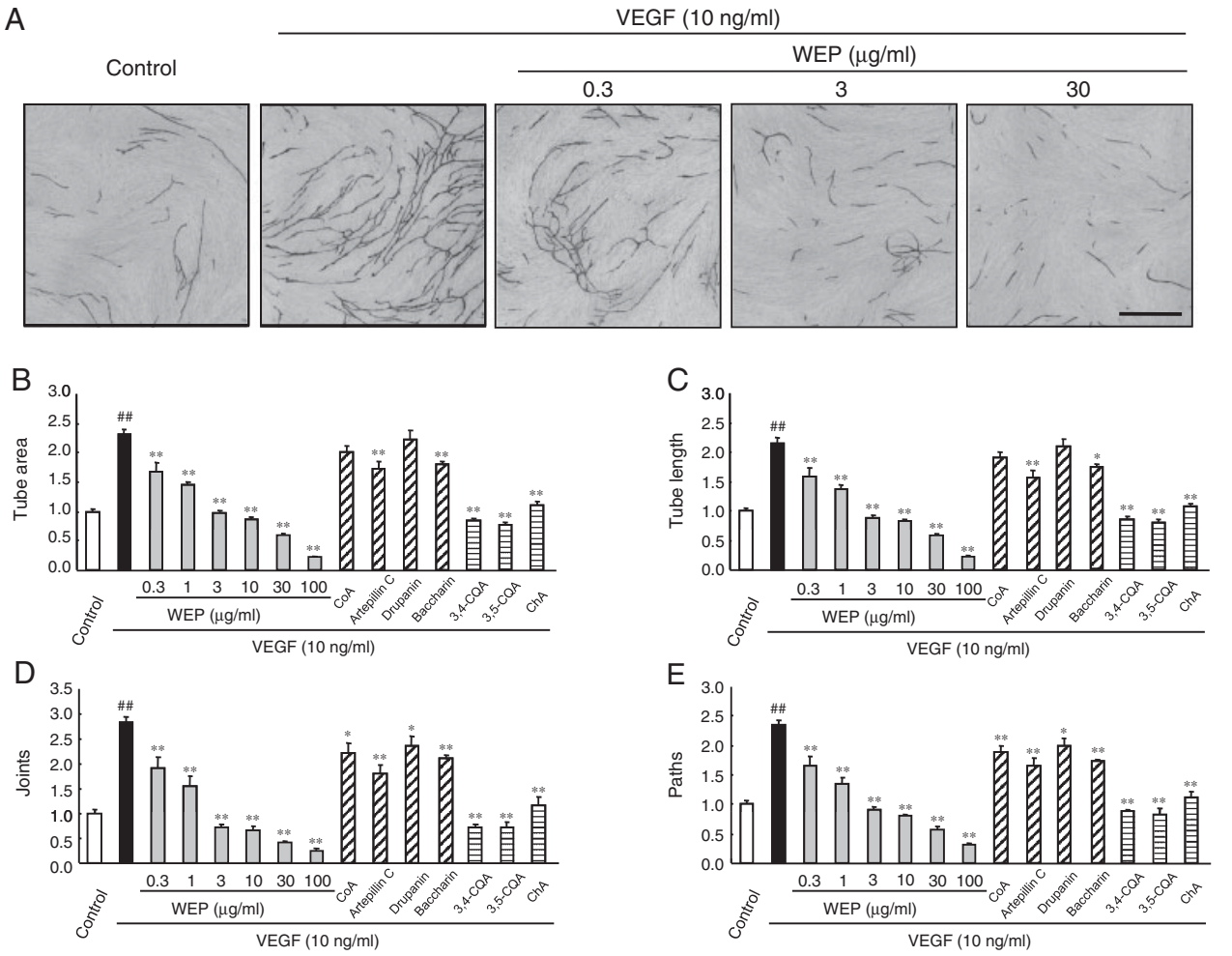

Figure 1. Effects of WEP and its main constituents on VEGF-induced HUVEC tube formation. (A) HUVECs were co-cultured with human fibroblasts, as described in Section 2. After cultivation for 11 days, HUVECs were stained with anti-CD31 antibody. Quantitative analysis of the stained tube-like structures was performed by an imaging analyzer (angiogenesis imaging analyzer, version 2) in five different fields for each well, measuring four parameters: (B) tube area, (C) tube length, (D) joints, and (E) paths. The concentrations of the WEP constituents were similar to those present in 100 μg/mL WEP (Table 1). Values are expressed as the mean ± SEM, with control values being given the value 1.0 ($n = 3$–9). $^{\#\#}p < 0.01$ *versus* control. $^{*}p < 0.05$, $^{**}p < 0.01$ *versus* VEGF alone. Scale bar, 1 mm.

3.2 Effect on cell proliferation

Tube formation is the final stage of angiogenesis and involves differentiation of endothelial cells to form new lumen-containing vessels. For a specific evaluation of vascular endothelial cell proliferation, a key initial step in angiogenesis, we examined whether WEP and caffeoylquinic acid derivatives (3,4-CQA, 3,5-CQA, and ChA) inhibited VEGF-induced HUVEC proliferation. In the VEGF-alone group, the proliferation of HUVECs (measured by WST-8 assay, see Section 2) was increased 2.1-fold (*versus* control). WEP suppressed this VEGF-induced HUVEC proliferation in a concentration-related manner, its effect being significant at concentrations of 30 μg/mL or more (Fig. 2A). On the other hand, three caffeoylquinic acid derivatives at 30 μM inhibited VEGF-induced HUVEC proliferation, but not at 10 μM (Fig. 2B).

3.3 Effect on cell migration

For a further investigation of the anti-angiogenic effects of WEP and caffeoylquinic acid derivatives, we tested their effects on vascular endothelial cell migration, an essential step in angiogenesis. For this we employed a wound-healing assay using HUVECs. The wound-healing assay is simple, inexpensive, and one of the earliest developed methods for the study of directional cell migration *in vitro*. Briefly, after starvation, confluent scrape-wounded HUVEC monolayers were incubated with WEP (3–100 μg/mL) or a caffeoylquinic acid derivative (3,4-CQA, 3,5-CQA, or ChA: 10–30 μM) in the presence of VEGF (10 ng/mL), and the number of cells that had migrated into the wound region was assessed 24 h later. In the VEGF-alone group, the number of migrated cells was increased 2.2-fold (*versus* the control group). WEP inhibited

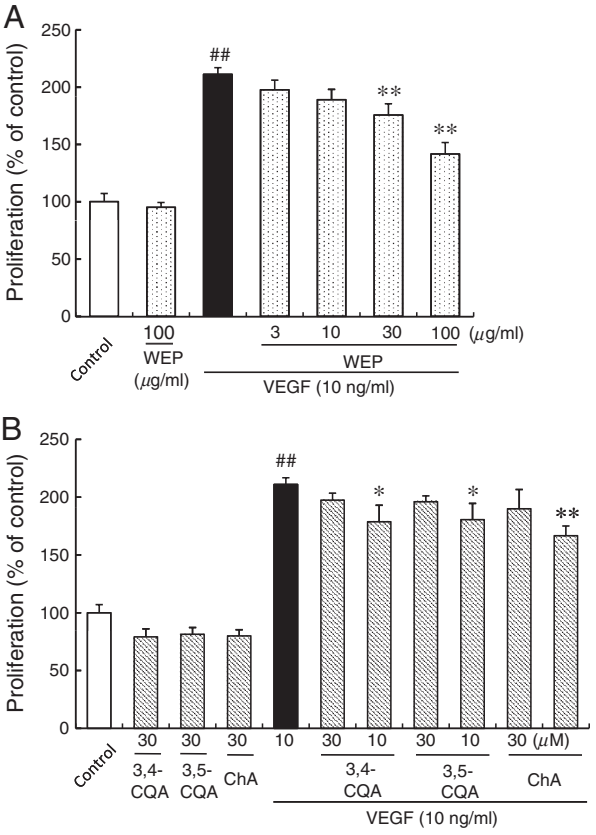

Figure 2. Effects of WEP and caffeoylquinic acid derivatives on VEGF-induced HUVEC proliferation. HUVECs were cultured in a 96-well plate (at a density of 2000 cells/well), and incubated for 72 h at 37°C in the presence or absence of VEGF (10 ng/mL) with or without either (A) WEP (3–100 μg/mL) or (B) various caffeoylquinic acid derivatives (3,4-CQA, 3,5-CQA, and ChA: 10, 30 μM). Numbers of viable cells were determined using the WST-8 assay, as described in Section 2. Values are expressed as the mean ± SEM ($n = 5$–17). $^{\#\#}p < 0.01$ *versus* control. $^{*}p < 0.05$, $^{**}p < 0.01$ *versus* VEGF alone.

this VEGF-induced HUVEC migration in a concentration-dependent manner, its effects being significant at concentrations of 10 μg/mL or more (*versus* VEGF-alone) (Figs. 3A and B). Application of 3,4-CQA, 3,5-CQA, or ChA concentration dependently reduced the number of migrated cells by about 20–35% (*versus* VEGF alone) (Fig. 3C).

3.4 MAPK pathway

To investigate the mechanism by which WEP and its caffeoylquinic acid derivatives suppressed *in vitro* tube formation, proliferation, and migration, we evaluated the phosphorylation levels of MAPK (ERK and p38) stimulated by VEGF in HUVECs using Western blotting. VEGF treatment increased the levels of phosphorylated ERK (p-ERK) and p38 (p-p38) by 3.8- and 2.9-fold, respectively. WEP (100 μg/mL) treatments with VEGF suppressed its phosphorylation of ERK and p38 (*versus* Vehicle) ($p < 0.01$) (Fig. 4). At 30 μM, 3,4-CQA also significantly suppressed VEGF-induced phosphorylation of ERK and p38 (*versus* Vehicle) ($p < 0.01$), but not at 10 μM (Fig. 4). On the other hand, single treatments of WEP or 3,4-CQA did not affect the phosphorylation of ERK and p38 (*versus* Control).

3.5 Effect on retinal neovascularizaton

To investigate the effects of WEP toward retinal neovascularization *in vivo*, we used an oxygen-induced retinopathy model in mice. WEP was subcutaneously administered at a daily dose of 300 mg/kg for 5 days starting immediately after the end of hyperoxia treatment (on P12). WEP suppressed the retinal neovascularization, which was observed as unregulated and abnormal vessel formation using fluorescein-conjugated dextran (Fig. 5A). Retinal neovascularization was evaluated by measuring the number of nodes and the nodes area (indexes of retinal neovascularization) using imaging software (see Section 2). The development of node regions (represented by green labels in each analyzed image) was suppressed by WEP treatment (*versus* Vehicle) (Fig. 5B). Furthermore, each of the measured parameters (the number of nodes and the nodes area) was significantly decreased by WEP treatment (*versus* Vehicle) (Figs. 5C and D), although revascularization in the capillary-free area did not differ between vehicle and WEP treatments (Fig. 5E).

3.6 Effect on body weight

To investigate the side effects of the above WEP treatment, we measured the body weights of the neonatal mice from the start of the treatment (P12) to the end-point (P17). On P12, the body weights (mean ± SD) of vehicle- and WEP-treated mice were 4.4 ± 1.1 and 4.4 ± 0.8 g, respectively, and on P17, they were 5.9 ± 0.8 and 6.1 ± 0.4 g, respectively. There were no significant differences in body weight between vehicle- and WEP-treated mice from P12 to P17. Systemic administration of WEP to the neonatal mice thus had no apparent adverse developmental effects, judging from their growth.

4 Discussion

In this study, we evaluated the effects of WEP and its major constituents against *in vitro* angiogenesis, and we also examined the effects of WEP in an *in vivo* angiogenesis model. In the *in vitro* study, WEP and its main constituents (caffeoylquinic derivatives 3,4-CQA, 3,5-CQA and ChA) inhibited VEGF-induced HUVEC tube formation, proliferation, and migration. Moreover, WEP and 3,4-CQA inhibited VEGF-stimulated phosphorylation of ERK and

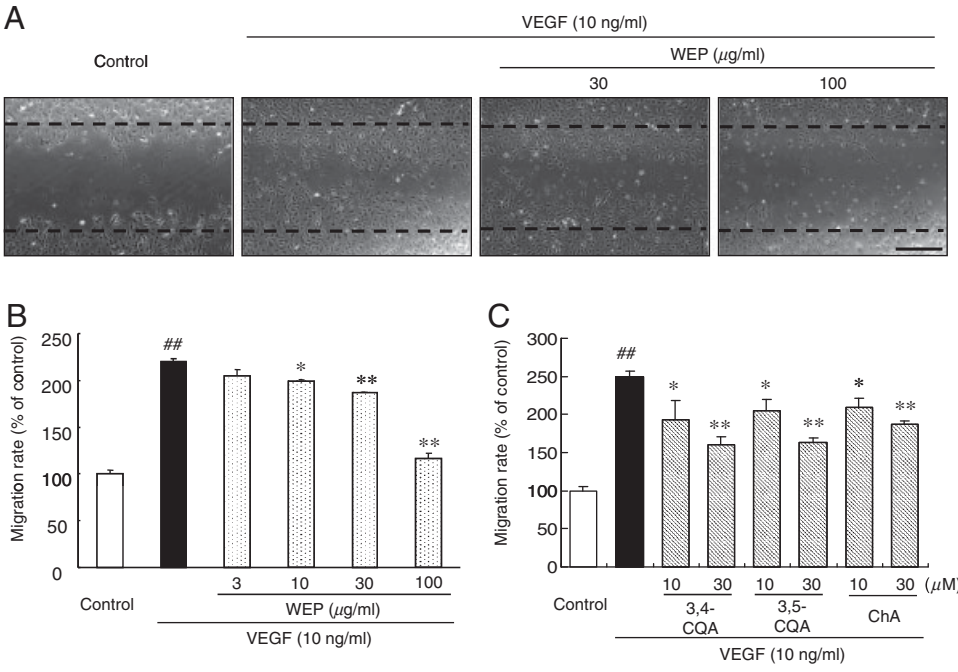

Figure 3. Effects of WEP and caffeoylquinic acid derivatives in an *in vitro* wound-healing assay. HUVEC migration was assessed using a wound-healing assay. Briefly, 90% confluent monolayers of HUVECs were scratched with a pipette tip, and treated for 24 h with VEGF (10 ng/mL) with or without either (B) WEP (3–100 μg/mL) or (C) various caffeoylquinic acid derivatives (3,4-CQA, 3,5-CQA, and ChA: 10, 30 μM). Migration was estimated by counting cell numbers within the wounded region. Broken lines indicate the wound edges. Values are expressed as the mean ± SEM ($n = 4$). $^{\#\#}p < 0.01$ *versus* control. $^{*}p < 0.05$, $^{**}p < 0.01$ *versus* VEGF alone. Scale bar, 500 μm.

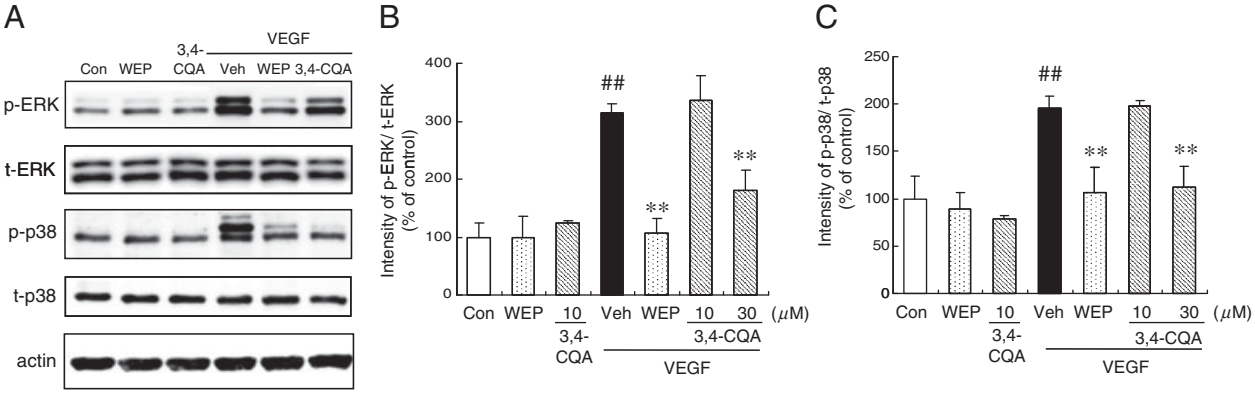

Figure 4. Effects of WEP and its caffeoylquinic acid derivative against VEGF signaling pathway. (A) HUVECs were treated with VEGF (10 ng/mL) with or without WEP (100 μg/mL) or 3,4-CQA (30 μM) for 5 min, and proteins isolated from HUVECs were separated on 10% SDS-PAGE and then subjected to immunoblot analysis for various antigens as indicated. Phosphorylation levels of (B) ERK and (C) p38 after treatment with VEGF (10 ng/mL) with or without WEP (100 μg/mL) or 3,4-CQA (10, 30 μM) for 5 min. These intensities were normalized with total ERK and total p38, respectively. Values are expressed as the mean ± SEM ($n = 3$–8). $^{\#\#}p < 0.01$ *versus* control. $^{**}p < 0.01$ *versus* VEGF alone.

p38. In the *in vivo* study, WEP suppressed the development of retinal neovascularization in a murine model of retinopathy without affecting the physiological revascularization.

To elucidate the anti-angiogenic effects of constituents present in WEP, we investigated their effects against VEGF-induced HUVEC tube formation, using each one at a concentration close to that in a 100 μg/mL solution of WEP (Table 1). The capacities of the various constituents to inhibit HUVEC tube formation are summarized in Table 2. The degree of inhibition induced by the various cinnamic acid derivatives (CoA, artepillin C, drupanin, and baccharin) was within the range 3–37%, whereas for the caffeoylquinic acid derivatives (3,4-CQA, 3,5-CQA and ChA) the range was 50–75% (*versus* VEGF alone). Since caffeoylquinic acid derivatives are in high concentrations in WEP and since their inhibitory effects against *in vitro* tube formation were stronger than those of the other constituents tested, the overall inhibitory effects of WEP may be mainly dependent on caffeoylquinic acid derivatives, at least against angiogenesis *in vitro*.

Angiogenesis is regulated by several growth factors, including basic fibroblasts growth factor, insulin-like growth factor 1, and VEGF. VEGF plays a particularly important

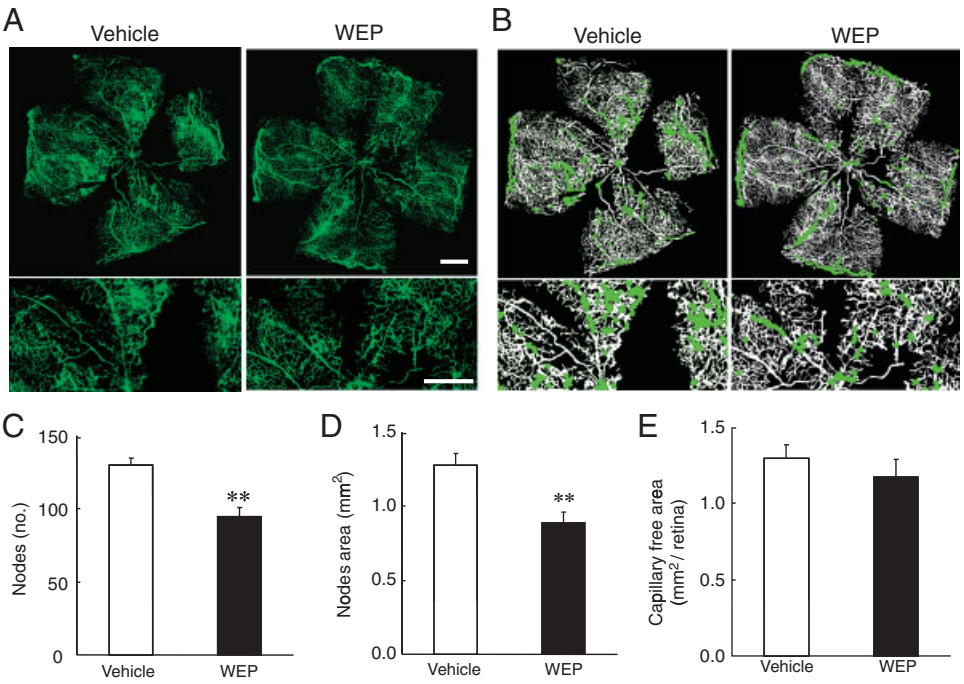

Figure 5. Effect of WEP on retinal neovascularization in a murine oxygen-induced retinopathy model. Original images (A) are shown, together with the analyzed images (B) obtained using the Angiogenesis Tube Formation module in Metamorph. The lower images show a higher-magnification version of part of the corresponding upper image. Green labels in analyzed images show the node regions. Scale bar, 500 μm. (C–E) Quantitative analysis was performed on the entire retinal microvasculature in flat-mounted retinas obtained at P17. WEP significantly decreased both the number of nodes (C) and the nodes area (D), which are indexes of pathological neovascularization (data were computed using the Angiogenesis Tube Formation module). Revascularization into the capillary-free area did not differ between vehicle and WEP (E). Values are expressed as the mean ± SEM ($n = 14$ or 15 animals *per* group). ''Vehicle'' means PBS. $^{**}p < 0.01$ *versus* vehicle.

role, and research into its role is being actively pursued. Downstream of the VEGF signaling pathway, phosphorylation of ERK and p38 lead to cell proliferation and migration, respectively [16, 17]. In this study, 3,4-CQA at 30 μM significantly suppressed cell proliferation, but not 10 μM (Fig. 2B). Similarly, 3,4-CQA at 30 μM inhibited VEGF-stimulated phosphorylation of ERK, but not 10 μM (Fig. 4B). On the other hand, VEGF-induced cell migration was suppressed by 3,4-CQA at 10 μM or more (Fig. 3C), but an effective concentration of 3,4-CQA against phosphorylation of p38 was 30 μM (Fig. 4C). However, HUVECs were incubated with VEGF and 3,4-CQA for 24 h in the wound-healing assay, but only 5 min in Western blot analysis. The difference of these effective concentrations may be caused by the duration of each experiment. Taken together, these results indicate that 3,4-CQA may inhibit VEGF-induced cell proliferation and migration by suppressing the phosphorylation of ERK and p38 in HUVECs.

Angiogenesis is an invasive process that requires proteolysis of the extracellular matrix and proliferation and migration of endothelial cells, as well as the synthesis of new matrix components. Matrix metalloproteinases, a family of extracellular endopeptidases, play an important role in the selective proteolysis of various components of extracellular matrix. A previous report indicates that ChA has a powerful inhibitory effect against matrix metalloproteinase-9 activities in a zymogelatin assay [24]. Therefore, ChA may play a pivotal role for cell migration. In fact, in this study, ChA suppressed the VEGF-induced migration. Moreover, 3,4-CQA, one of the caffeoylquinic acid derivatives, suppressed the VEGF-induced phosphorylation of p38 as well as WEP. From these results, caffeoylquinic acid may become a useful agent for suppression of cell migration.

Artepillin C at 11–176 μM reportedly displays anti-angiogenic effects against HUVEC tube formation and proliferation, as well as in a mouse dorsal air sac assay [25]. Similarly, in the present study, artepillin C had a suppressive effect on VEGF-induced HUVEC tube formation, although this *in vitro* effect was weak. We suspect that the reason for the effect being weak was the low concentration (2.0 μM) of artepillin C used in this study. We used such a low concentration because our policy was to use each of the WEP constituents at a concentration close to that present in a 100 μg/mL solution of WEP.

Propolis exerts a variety of pharmacological actions such as anti-tumor and anti-inflammatory effects. In the field of ophthalmology, beneficial effects of propolis have been reported in various experimental models *in vivo*. These include: an

Table 2. Inhibitory capacities of WEP main constituents against VEGF-induced HUVEC tube formation[a)]

	CoA	Artepilin C	Drupanin	Baccharin	3,4-CQA	3,5-CQA	ChA
Tube area	–	+	+	–	+++	+++	+++
Tube length	–	+	+	–	+++	+++	+++
Joints	+	++	+	+	+++	+++	+++
Paths	+	++	+	+	+++	+++	+++

a) The degree of inhibition induced by each WEP constituent against the effect of VEGF alone on a given each parameter (tube area, tube length, joints, or paths) is indicated as follows:–, 0–15% (no effect);+, 15–30%; ++, 30–45%; and +++, more than 45%.

endotoxin-induced uveitis model [26], a bacteria (*Pseudomonas aeruginosa* and *Staphylococcus aureus*)- or *Acanthamoeba*-infected keratitis model [27–29], a silver nitrate cauterization-injured cornea neovascularization model [19], a corneal epithelial wound-healing model induced either by alkali burn or by mechanical scraping [30, 31], a selenite-induced cataract model [32], and an N-methyl-D-aspartate-induced retinal damage model [33]. However, this is the first report of anti-angiogenic effects of WEP against retinal neovascularization in a murine oxygen-induced retinopathy model.

Reactive oxygen species is one of the causative substances inducing oxidative stress and treatment with an antioxidant (*N*-acetyl-cysteine, *N, N'*-dimethylthiourea, or vitamin C or E) has been shown to cause a suppression of VEGF expression *in vitro* [34–37]. Moreover, treatment with trolox (a vitamin E analog) has been shown to suppress retinal neovascularization in a rat oxygen-induced retinopathy model [38]. A few years ago we reported that WEP has anti-oxidative effects (*i.e.* it inhibited lipid peroxidation in mouse forebrain homogenates) [39]. The reported effective anti-oxidative concentrations of WEP (0.02–20 μg/mL) are fairly well in line with in those found in the present study (0.3–100 μg/mL) to be effective against *in vitro* tube formation. On that basis, the mechanism responsible for the present anti-angiogenic effects of WEP may overlap (in whole or in part) with that responsible for its anti-oxidative effects. However, that idea is speculative at present, and further investigations will be needed to test it.

In conclusion, our data indicate that WEP has anti-angiogenic effects both *in vitro* and *in vivo*. Further, its major constituents (caffeoylquinic acid derivatives) also have angiostatic effects *in vitro*. The angiostatic effects of WEP and 3,4-CQA may be, in part, dependent on its inhibitory effects of VEGF-stimulated MAPK pathway. These observations should help in the development of useful therapeutic agents for diseases involving neovascularization, such as retinal neovascular diseases.

The authors thank Dr. Kazumichi Suzuki for providing artepillin C, baccharin, drupanin, 3,4-CQA, 3,5-CQA, and WEP.

The authors have declared no conflict of interest.

5 References

[1] Bankova, V., Marcucci, M. C., Simova, S., Nikolova, N. *et al.*, Antibacterial diterpenic acids from Brazilian propolis. *Z. Naturforsch. [C]* 1996, *51*, 277–280.

[2] Drago, L., Mombelli, B., De Vecchi, E., Fassina, M. C. *et al.*, *In vitro* antimicrobial activity of propolis dry extract. *J. Chemother.* 2000, *12*, 390–395.

[3] Mirzoeva, O. K., Calder, P. C., The effect of propolis and its components on eicosanoid production during the inflammatory response. *Prostaglandins Leukot. Essent. Fatty Acids* 1996, *55*, 441–449.

[4] Matsuno, T., Isolation and characterization of the tumoricidal substance from Brazilian propolis. *Honeybee Sci.* 1992, *13*, 49–54.

[5] Chen, C. N., Weng, M. S., Wu, C. L., Lin, J. K., Comparison of radical scavenging activity, cytotoxic effects and apoptosis induction in human Melanoma cells by Taiwanese propolis from different sources. *Evid. Based Complement. Alternat. Med.* 2004, *1*, 175–185.

[6] Greenaway, W., May, J., Scaysbrook, T., Whatley, F. R., Identification by gas chromatography-mass spectrometry of 150 compounds in propolis. *Zeitschrift für Naturforschung C* 1991, *46*, 111–121.

[7] Marcucci, M. C., Propolis: chemical composition, biological properties and therapeutics activity. *Apidologie* 1995, *26*, 83–99.

[8] Bankova, V. S., de Castro, S. L., Marcucci, M. C., Propolis: recent advances in chemistry and plant origin. *Apidologie* 2000, *31*, 3–15.

[9] Kujumgiev, A., Tsvetkova, I., Serkedjieva, Y., Bankova, V. *et al.*, Antibacterial, antifungal and antiviral activity of propolis of different geographic origin. *J. Ethnopharmacol.* 1999, *64*, 235–240.

[10] Markham, K. E., Mitchel, K. A., Wilkins, A. L., Daldy, J. A., Lu, Y., HPLC and GC-MS identification of the major organic constituents in New Zealand propolis. *Phytochemistry* 1996, *42*, 205–211.

[11] Midorikawa, K., Banskota, A. H., Tezuka, Y., Nagaoka, T. *et al.*, Liquid chromatography-mass spectrometry analysis of propolis. *Phytochem. Anal.* 2001, *12*, 366–373.

[12] Park, Y. K., Alencar, S. M., Aguiar, C. L., Botanical origin and chemical composition of Brazilian propolis. *J. Agric. Food Chem.* 2002, *50*, 2502–2506.

[13] Kumazawa, S., Yoneda, M., Shibata, I., Kanaeda, J. *et al.*, Direct evidence for the plant origin of Brazilian propolis by the observation of honeybee behavior and phytochemical analysis. *Chem. Pharm. Bull. (Tokyo)* 2003, *51*, 740–742.

[14] Kumazawa, S., Yoneda, M., Nakayama, T., Constituents in Brazilian propolis and its plant of origin. *Foods Food Ingredient J. Jpn.* 2004, *209*, 132–139.

[15] Teixeira, E. W., Negri, G., Meira, R. M., Message, D., Salatino, A., Plant origin of green propolis: bee behavior, plant anatomy and chemistry. *Evid. Based Complement. Alternat. Med.* 2005, *2*, 85–92.

[16] Meadows, K. N., Bryant, P., Pumiglia, K., Vascular endothelial growth factor induction of the angiogenic phenotype requires Ras activation. *J. Biol. Chem.* 2001, *276*, 49289–49298.

[17] Rousseau, S., Houle, F., Kotanides, H., Witte, L. *et al.*, Vascular endothelial growth factor (VEGF)-driven actin-based motility is mediated by VEGFR2 and requires concerted activation of stress-activated protein kinase 2 (SAPK2/p38) and geldanamycin-sensitive phosphorylation of focal adhesion kinase. *J. Biol. Chem.* 2000, *275*, 10661–10672.

[18] Song, Y. S., Park, E. H., Jung, K. J., Jin, C., Inhibition of angiogenesis by propolis. *Arch. Pharm. Res.* 2002, *25*, 500–504.

[19] Hepsen, I. F., Er, H., Cekic, O., Topically applied water extract of propolis to suppress corneal neovascularization in rabbits. *Ophthalmic Res.* 1999, *31*, 426–431.

[20] Mishima, S., Narita, Y., Chikamatsu, S., Inoh, Y. *et al.*, Effects of propolis on cell growth and gene expression in HL-60 cells. *J. Ethnopharmacol.* 2005, *99*, 5–11.

[21] Izuta, H., Chikaraishi, Y., Shimazawa, M., Mishima, S. *et al.*, 10-Hydroxy-2-decenoic acid, a major fatty acid from royal jelly, inhibits VEGF-induced angiogenesis in human umbilical vein endothelial cells. *Evid. Based Complement. Alternat. Med.* 2007, doi: 0.1093/ecam/nem 152.

[22] Smith, L. E., Wesolowski, E., McLellan, A., Kostyk, S. K. *et al.*, Oxygen-induced retinopathy in the mouse. *Invest. Ophthalmol. Vis. Sci.* 1994, *35*, 101–111.

[23] Chikaraishi, Y., Shimazawa, M., Hara, H., New quantitative analysis, using high-resolution images, of oxygen-induced retinal neovascularization in mice. *Exp. Eye Res.* 2007, *84*, 529–536.

[24] Jin, U. H., Lee, J. Y., Kang, S. K., Kim, J. K. *et al.*, A phenolic compound, 5-caffeoylquinic acid (chlorogenic acid), is a new type and strong matrix metalloproteinase-9 inhibitor: isolation and identification from methanol extract of *Euonymus alatus*. *Life Sci.* 2005, *77*, 2760–2769.

[25] Ahn, M. R., Kunimasa, K., Ohta, T., Kumazawa, S. *et al.*, Suppression of tumor-induced angiogenesis by Brazilian propolis: major component artepillin C inhibits *in vitro* tube formation and endothelial cell proliferation. *Cancer Lett.* 2007, *252*, 235–243.

[26] Ozturk, F., Kurt, E., Inan, U. U., Emiroglu, L. *et al.*, Effect of propolis on endotoxin-induced uveitis in rabbits. *Jpn. J. Ophthalmol.* 1999, *43*, 285–289.

[27] Oksuz, H., Duran, N., Tamer, C., Cetin, M., Silici, S., Effect of propolis in the treatment of experimental *Staphylococcus aureus* keratitis in rabbits. *Ophthalmic Res.* 2005, *37*, 328–334.

[28] Onlen, Y., Tamer, C., Oksuz, H., Duran, N. *et al.*, Comparative trial of different anti-bacterial combinations with propolis and ciprofloxacin on Pseudomonas keratitis in rabbits. *Microbiol. Res.* 2007, *162*, 62–68.

[29] Vural, A., Polat, Z. A., Topalkara, A., Toker, M. I. *et al.*, The effect of propolis in experimental Acanthamoeba keratitis. *Clin. Experiment. Ophthalmol.* 2007, *35*, 749–754.

[30] Ozturk, F., Kurt, E., Inan, U. U., Emiroglu, L. *et al.*, The effects of acetylcholine and propolis extract on corneal epithelial wound healing in rats. *Cornea* 1999, *18*, 466–471.

[31] Ozturk, F., Kurt, E., Cerci, M., Emiroglu, L. *et al.*, The effect of propolis extract in experimental chemical corneal injury. *Ophthalmic Res.* 2000, *32*, 13–18.

[32] Orhan, H., Marol, S., Hepsen, I. F., Sahin, G., Effects of some probable antioxidants on selenite-induced cataract formation and oxidative stress-related parameters in rats. *Toxicology* 1999, *139*, 219–232.

[33] Inokuchi, Y., Shimazawa, M., Nakajima, Y., Suemori, S. *et al.*, Brazilian green propolis protects against retinal damage *in vitro* and *in vivo*. *Evid. Based Complement. Alternat. Med.* 2006, *3*, 71–77.

[34] Chua, C. C., Hamdy, R. C., Chua, B. H., Upregulation of vascular endothelial growth factor by H2O2 in rat heart endothelial cells. *Free Radic. Biol. Med.* 1998, *25*, 891–897.

[35] Lu, M., Kuroki, M., Amano, S., Tolentino, M. *et al.*, Advanced glycation end products increase retinal vascular endothelial growth factor expression. *J. Clin. Invest.* 1998, *101*, 1219–1224.

[36] Redondo, P., Bandres, E., Solano, T., Okroujnov, I., Garcia-Foncillas, J., Vascular endothelial growth factor (VEGF) and melanoma. N-acetylcysteine downregulates VEGF production *in vitro*. *Cytokine* 2000, *12*, 374–378.

[37] Rodriguez, J. A., Nespereira, B., Perez-Ilzarbe, M., Eguinoa, E., Paramo, J. A., Vitamins C and E prevent endothelial VEGF and VEGFR-2 overexpression induced by porcine hypercholesterolemic LDL. *Cardiovasc. Res.* 2005, *65*, 665–673.

[38] Penn, J. S., Tolman, B. L., Bullard, L. E., Effect of a water-soluble vitamin E analog, trolox C, on retinal vascular development in an animal model of retinopathy of prematurity. *Free Radic. Biol. Med.* 1997, *22*, 977–984.

[39] Shimazawa, M., Chikamatsu, S., Morimoto, N., Mishima, S. *et al.*, Neuroprotection by Brazilian green propolis against *in vitro* and *in vivo* ischemic neuronal damage. *Evid. Based Complement. Alternat. Med.* 2005, *2*, 201–207.

